Regenerative Braking and Rapid Acceleration System for Electric Vehicles using Integrated Battery and Supercapacitor

Mahamad Nabab Alam
Department of Electrical Engineering
National Institute of Technology Warangal
Warangal-506004, India
mnalam@nitw.ac.in

2024 IEEE 4th International Conference on Sustainable Energy and Future Electric Transportation (SEFET) | 979-8-3503-8399-7/24/$31.00 ©2024 IEEE | DOI: 10.1109/SEFET61574.2024.10718265

***Abstract*—This research explores the integration of batteries and supercapacitors in a Hybrid Energy Storage System (HESS) for Electric Vehicles (EVs), leveraging their complementary characteristics. The proposed system aims to enhance vehicle acceleration, battery safety, and efficiency of the regenerative braking system (RBS). A novel regenerative braking and rapid acceleration system is introduced, driven by a brushless DC (BLDC) motor. During regenerative braking, the BLDC functions as a generator, transferring energy to either the supercapacitor or the battery based on specified current requirements and storage system capabilities. Harvested energy improves acceleration and prevents deep discharging of the battery during uphill driving or rapid charging during downhill or high braking situations. The supercapacitor plays a crucial role due to its efficient charging, energy storage during braking, and rapid energy release during acceleration. PID controllers and power electronic switches manage power distribution for reliable braking and acceleration, while a PI controller adjusts braking current as per torque needs. Extensive simulations and experiments validate the efficacy of the proposed system, affirming its capability for high-performance operation in real-world scenarios.**

***Index Terms*—acceleration system, battery, supercapacitor, brushless DC motor, regenerative braking, electric vehicle.**

I. Introduction

Over the past few years, there has been a substantial uptick in the adoption of electric propulsion within road transport, encompassing a variety of technologies such as internal combustion engine hybrids, battery electric vehicles, and fuel cell vehicles. Among these, spark ignition engine hybrids stand out as the most prevalent. Electric vehicles (EVs) are increasingly under the spotlight due to their distinctive advantages, including minimal emissions, heightened efficiency, and silent operation.

Chemical batteries have historically served as the primary energy storage system (ESS) across numerous industrial sectors. They hold sway as the dominant technology within the electric car industry. Nevertheless, chemical batteries have several limitations, including restricted cycle life, suboptimal power density, and steep costs. This has given rise to a regenerative braking system (RBS), wherein a vehicle's kinetic energy is harnessed and stored as electric energy during braking, repurposed to extend the range of battery-electric vehicles. To effectively harness this energy, some form of energy storage is essential, typically realized through batteries and supercapacitors [1].

979-8-3503-8399-7/24/$31.00 ©2024 IEEE

Batteries remain the favoured option owing to their extensive integration into hybrid and electric vehicles. However, they grapple with challenges related to high-power transient charging during braking, which can significantly impact performance and longevity. Supercapacitors (SC) exhibit outstanding power densities, efficiently capturing the energy produced during braking and demonstrating excellent cycling performance [2].

Supercapacitors have garnered significant attention as electrochemical devices designed to bridge the gap between traditional capacitors, which typically offer low energy density, and batteries, which often suffer from low power density. The electrostatic charging mechanism inherent in supercapacitors, characterized by two parallel plates separated by an electrolyte, has positioned the electrical double-layer capacitor (EDLC) as a formidable contender against conventional capacitors. This is primarily due to advancements in optimizing electrode surface area, electrode separation distance, and exploring various electrolytes. Despite these advancements, supercapacitors still face challenges related to energy density compared to batteries. Consequently, ongoing research focuses on developing new electrode materials and electrolyte mediums and refining the configuration and packaging of supercapacitor systems.

In the realm of EVs, extensive efforts have been directed towards leveraging supercapacitors to address the limitations of traditional batteries. One prevalent approach involves integrating supercapacitors into hybrid energy storage systems (HESSs), particularly in the supercapacitor/battery topology, where the battery pack is directly linked to the DC bus. A bidirectional DC/DC converter governs the power exchange between the battery and supercapacitor. However, the requirement for two distinct energy storage systems and an additional power converter often undermines the cost-effectiveness of HESSs. Furthermore, ensuring optimal utilization of the supercapacitor's capabilities necessitates matching the power level of

the supercapacitor module with the bidirectional converter, thereby increasing overall system costs.

To address these challenges, a novel HESS architecture is proposed, integrating a supercapacitor module, battery pack, and current and speed controllers. Various operational modes of this proposed HESS are elaborated upon, and a new RBS is introduced. During braking, the DC-link voltage is boosted using a tailored switching algorithm within the inverter, adjusting the pulse width modulation (PWM) duty cycle to regulate the DC-link voltage. Consequently, regenerative braking can be achieved using the battery pack when the supercapacitor nears full charge. This innovative approach enhances regenerative braking efficiency and eliminates the need for dedicated converters, contributing to overall system optimization [3].

II. Supercapacitor (SC)

Supercapacitors represent advanced electronic devices designed to store vast amounts of electrical charge, also called double-layer or ultracapacitors. Unlike conventional capacitors, supercapacitors utilize two distinct mechanisms for storing electrical energy: double-layer capacitance and pseudo-capacitance. Double-layer capacitance operates on an electrostatic basis, while pseudo-capacitance functions on an electrochemical level, effectively combining the characteristics of standard capacitors with those of conventional batteries. This technology allows for capacitances reaching as high as 12000 F.

Unlike ordinary electrostatic capacitors, which may accommodate high maximum operating voltages, supercapacitors typically exhibit maximum charge voltages ranging between 2.5 to 2.7 volts. As polar devices, supercapacitors necessitate correct circuit connection, akin to electrolyte capacitors.

The unique characteristics of supercapacitors play a pivotal role in selecting the appropriate device for specific applications [4], [5]. In the ensuing discussion, we delve into the electrical ramifications, elucidating the primary electrical phenomena and assessing their influence on supercapacitor performance within energy systems. Depending on the distinct requirements of each application, particular attention may need to be directed towards specific aspects.

A. Self Discharge

Concise the following contents in one paragraph: Self-discharge affects all capacitors, including supercapacitors, by gradually reducing the voltage in a fully charged cell due to a constant leakage current in an open-circuit cell. This phenomenon diminishes the deliverable power and energy of supercapacitors, posing a significant challenge for commercial applications. Thermodynamic instability in the charged state can lead to self-discharge, exceeding the electrolyte's thermodynamic limit and causing Faradaic decomposition of the solution. Supercapacitors experience self-discharge due to ion redistribution within electrode pores and rapid charging behaviour. Excess ions migrate to adjacent pores, leading to voltage decay. To study self-discharge, fully charged supercapacitors are left idle and monitored for voltage drop, lasting from minutes to weeks. Self-discharge risk from Faradic reactions can be mitigated using organic electrolytes and assembling cells in a moisture-free environment.

B. Cyclability

Supercapacitors are notable for their cycle stability, often demonstrating long-life cycles exceeding half a million in commercial applications. Lab-scale testing typically involves 1000 to 10,000 cycles, each comprising a charge/discharge cycle at a constant current density. Extended cycling can lead to electrode degradation and component corrosion, reducing capacitance and increasing equivalent series resistance (ESR). Comparing initial and final performance from cycle testing offers insight into material performance under real-world conditions with high cycle counts.

C. High Frequency Behaviour

Supercapacitors excel in applications requiring fast charge-discharge cycles, unlike batteries, which suffer damage under such conditions. However, due to ion passage limitations through the electrolyte, supercapacitors cannot handle frequencies as high as conventional capacitors. Typically, there's a cut-off frequency, around 1 Hz, beyond which capacitance drastically decreases. Consequently, supercapacitors cannot filter high-frequency harmonic components of electronic converters, typically several kHz.

Nevertheless, there are applications, like filtering diode rectifier harmonics in the hundreds of Hertz range, where supercapacitors have been investigated. Research suggests that a grid of 25 electrodes is required for usable capacity in this frequency range. Therefore, the cut-off frequency for a graphene supercapacitor lies in the hundreds of Hz range.

D. Power and Energy Densities

Energy densities: Specific energy density (watt-hour per kilogram) is expressed by

$$ED = \frac{1}{2} C_s (\Delta V)^2 = \frac{1}{2} \frac{C}{m} (\Delta V)^2 \tag{1}$$

In the above equation, C_s represents specific capacitance obtained from cyclic voltammetry (CV) or galvanostatic charge-discharge (GCD) techniques, and ΔV denotes the operating potential range. The latter part of the equation links specific energy density to total capacitance (C) and active materials mass (m). The squared potential range emphasizes the significant impact of the operating voltage window on energy density. The choice of electrolyte determines the operating potential range in supercapacitors. However, transitioning to electrolytes with a broader voltage window may lead to a reduction in power density.

Power Densities: Specific power density (watt per kilogram) quantifies how rapidly a device can transfer energy to external loads under constant current density conditions.

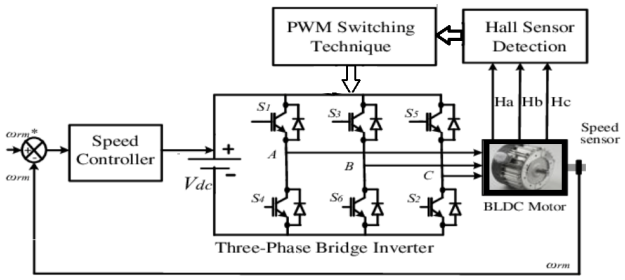

Fig. 1. BLDC and inverter connection.

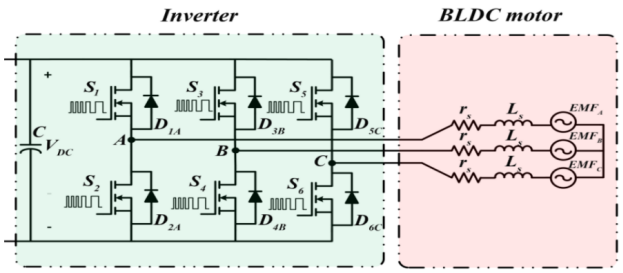

Fig. 2. BLDC and inverter connection description [6].

The maximum specific power density is determined as follows:

$$PD_{max} = \frac{(\Delta V)^2}{2mR_{ESR}} \tag{2}$$

In the above equation, ΔV represents the potential range, m stands for the mass of the active materials, and R_{ESR} denotes the cell's ESR. The ESR encompasses electrolyte ohmic resistance, cell design resistance, and additional resistances. Using organic or ionic liquids (ILs) as electrolytes can expand the voltage window, yet their lower ionic conductivities lead to increased R_{ESR}, thereby compromising overall power performance. The maximum power can be determined by averaging through a clear relationship between specific energy density and average specific power density, yielding.

$$PD_{avg} = \frac{ED}{\Delta t} \tag{3}$$

where Δt is the rate of discharge of the cell.

III. Inverter Based BLDC

A brushless DC motor is an electronically commutated DC motor with no brushes [6]. A controller is connected to the BLDC motor, which gives electric pulses to the three windings inside the stator and helps control the speed and torque of the synchronous motor. In construction, it is similar to a permanent magnet synchronous motor (PMSM) where the rotor is made of permanent magnets and the stator has three-phase winding. The only difference is in PMSM; the Voltage given is a three-phase AC, and in the case of BLDC, the source is the stream of current pulses, as shown in Fig. 1.

Motoring mode: In a BLDC drive, there are hall sensors that detect the position of the rotor based on the magnetic field inside the rotor, and that information is sent to the control logic. The control logic decodes it, compares it with the speed required, and supplies the gate pulses accordingly so that the rotor speed can achieve the reference speed. This design has a phase with a positive and negative constant current at any given time. The flux of this current produces attracts and repels the rotor, producing the required torque.

Generating mode: In regenerative braking, the BLDC machine functions as a generator, allowing the vehicle's kinetic energy to be stored in the HESS by reversing current flow. To enable this, the DC-link voltage requires boosting. Under normal conditions, the inverter's six switches are commutated based on rotor position determined by Hall effect sensors. However, during regenerative braking, the high-side switches of the half-bridge are all deactivated, and PWM regulates the low-side MOSFETs using a suitable switching scheme. This mode entails six commutation intervals, with only one inverter switch activated and deactivated during each interval, as depicted in Fig. 2.

Suppose S_2 is on for a time interval t_{on}. The current ramps up linearly in $2L_s$ to a peak value

$$I_p = (V_{emf} \times t_{on})/L_s \tag{4}$$

Therefore, the amount of the stored energy in the inductor can be represented as:

$$E = \frac{1}{2}(2L_s) \times I_p^2 = L_s I_p^2 \tag{5}$$

When S_2 is activated, the output is exclusively sourced from C, chosen sufficiently large to sustain the output during the time interval t_{on} with minimal voltage drop. Upon deactivating S_2, D_{1a} becomes forward biased, enabling the utilization of both back-EMFs and stored energy in the inductor to supply the supercapacitor. In this scenario, the PI controller regulates the output voltage by adjusting the on-time of S_2 within a negative feedback loop. If all energies could be fully transferred to the output during each period T (assuming 100 per cent conversion efficiency), the power transferred to the load from $2L_s$ would be:

$$P_{inductor} = \frac{L_s I_p^2}{T}\omega \tag{6}$$

Furthermore, a quantity of power P_{DC} is conveyed to the output from $2V_{emf}$, expressed as:

$$P_{DC} = 2V_{emf}\frac{I_p}{2} \times \frac{T_r}{T} \tag{7}$$

With T_r denoting the duration until the current in the inductor reaches zero, the resultant power transmitted to the load can be determined accordingly:

$$P_{total} = P_{inductor} + P_{DC} \tag{8}$$

After substituting I_p:

$$P_{total} = \frac{V_{emf}^2 \times t_{on}}{L_s \times T}(t_{on} + t_r) \tag{9}$$

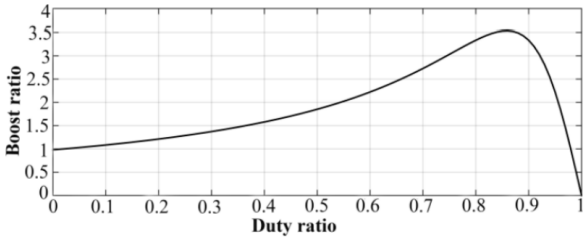

Fig. 3. Duty ratio Vs boost ratio.

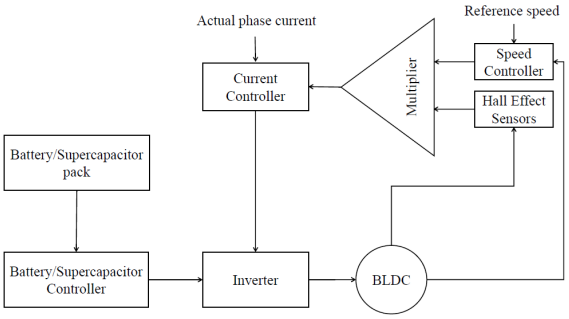

Fig. 4. Block diagram of the proposed model.

The circuit is assumed to operate in discontinuous mode, thus $t_{on} + t_r = mT$ in which m is a fraction less than 1. This equation can be restated as:

$$P_{total} = \frac{V_{emf}^2 \times t_{on}}{L_s \times T}(mT) = \frac{V_{DC}^2}{R} \tag{10}$$

Here, R denotes the output resistance. Through certain adjustments, the conversion ratio is derived as follows:

$$\frac{V_{DC}}{V_{emf}} = \sqrt{\frac{R \times t_{on} \times m}{L_s}} \tag{11}$$

Fig. 3 plots the conversion ratio versus the duty cycle.

IV. Proposed Regenerative Braking Approach

Regenerative braking and rapid acceleration systems integrating SC and battery are discussed here.

Fig. 4 shows the block diagram of the proposed model. The BLDC is connected to the 6-pulse inverter, which converts the current from the supercapacitor and battery pack to a stream of current pulses and gives it to the BLDC. The hall effect sensors in the BLDC sense the position of the rotor using the magnetic field inside it and provide it to the multiplier [7], [8].

The hall effect sensor only provides the position, so a decoder is used to decode the position and get the sequence of excitation needed for the three phases of the BLDC. A speed controller compares the reference and actual speeds and controls the error using a PI controller. The output of the speed controller is the reference current needed to attain the reference speed. This reference current is multiplied by the hall effect sensor output to get the reference currents required in the three phases of the BLDC. These three reference currents are given to the current controller, where the reference currents are compared with the actual currents in the BLDC, and gate pulses are generated according to the error between the reference currents and actual currents. These gate pulses are then given to the inverter.

TABLE I
Specifications of the Used Equipment

S.no	Device	Specifications
1	Li-ion Battery	Capacity: 86Ah, 4.386KWh Voltage = 51V Peak discharging current = 20A Peak charging current = 10A
2	Supercapacitor (BCAP0350)	Rated Capacitance = 350F ESR = 3.2mΩ Rated Voltage = 2.7V/2.5V Specific Power = 4600W/kg Specific Energy = 5.9Wh/kg Peak current = 840A
3	BLDC motor	Rated Power = 4.5KW Stator resistance = 9.5mΩ

The battery and supercapacitor pack are connected to the inverter through a controller that shares the load between the two sources according to the currents. The controller action is such that when the current from the battery goes above a certain value, the controller switches the supply from the battery to the supercapacitor, which can handle large currents.

Similarly, when the charging current goes above a certain value during braking, the controller switches the source from the battery to the supercapacitor. Again, when the current comes in the acceptable range, the Controller switches back the source from the supercapacitor to the battery. This switching action increases the battery life and cyclability and can deal with huge currents during rapid acceleration or braking.

Fig. 5 is the complete design for the HESS model proposed for the regenerative braking and rapid acceleration system. The battery/SC controller switches the load according to the current in the DC link, which is discussed in depth in the following sections. The controller in the figure takes the hall sensor output, reference speed, and phase currents and converts them to the gate pulses given to the inverter.

The equipment used in the simulation study is specified in Table I. This table gives all the necessary data considered for performing the proposed study.

V. Results and Discussions

The simulation results from Simulink, mainly the current, SOC, voltage and speed results, and the results for various components are also presented in this section.

In Fig. 6, the reference and actual speeds of the BLDC are observed, with the actual speed demonstrating precise tracking of the reference speed, indicative of effective speed control of the BLDC motor. In Fig. 7, the load torque applied to the BLDC motor is depicted, simulating various road elevations and loads, with the consistent aim of maintaining motor speed identical to the reference speed across all load variations. Fig. 6 portrays the battery's state of charge (%SOC), exhibiting fluctuations suggestive of its charging and discharging cycles. Meanwhile, Fig. 9 delineates the current flowing into the battery, where

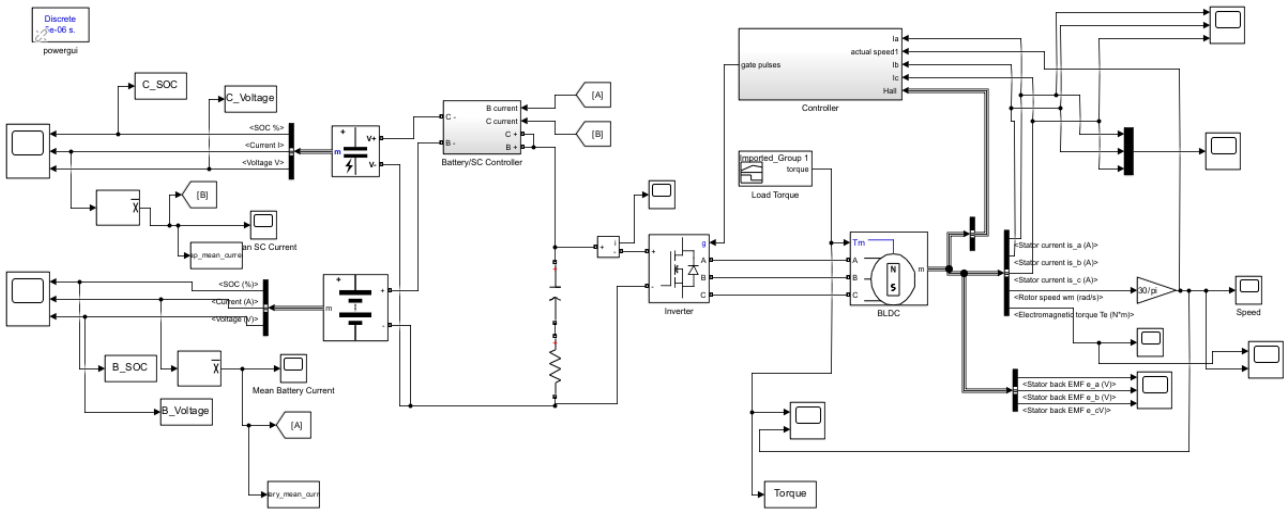

Fig. 5. Simulink simulation blocks of the proposed model.

negative values denote charging and positive values indicate discharging, with deviations beyond 20 A attributed to switching between the supercapacitor and battery. The battery current remains within -10 A to 20 A bounds outside switching instances. The behaviour of the battery's terminal voltage remains relatively constant, as illustrated in Fig. 10, with transient drops observed during switching.

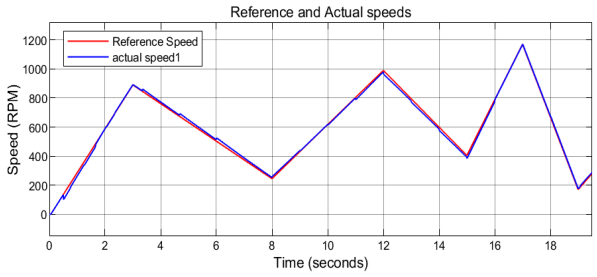

Fig. 6. Reference speed Vs Actual speed.

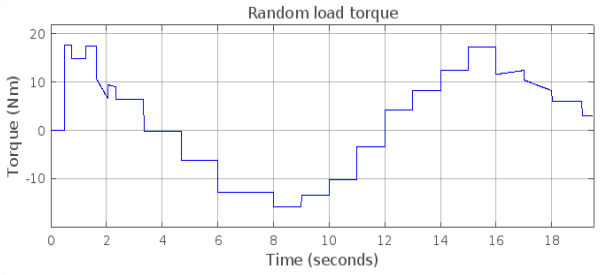

Fig. 7. Load torque.

Similarly, Fig. 11 showcases the %SOC of the supercapacitor, depicting its charging and discharging patterns. In contrast, Fig. 12 presents the current state of the SC, consistently operating within high-power regimes, as evidenced by currents exceeding 20 A or falling below -10 A. Finally, Fig. 13 displays the terminal voltage behaviour of the SC, maintaining stability with transient

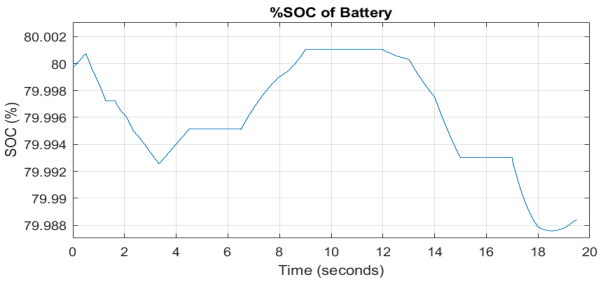

Fig. 8. %SOC of battery.

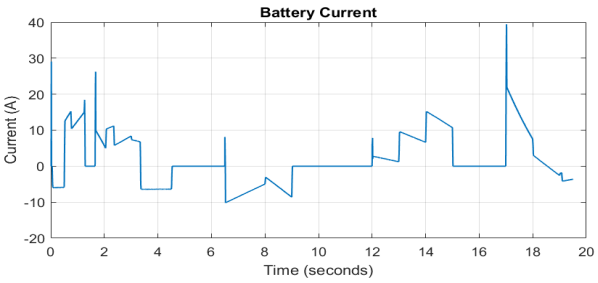

Fig. 9. Current in the battery.

voltage spikes during switching events. These comprehensive observations provide valuable insights into the dynamic performance and control strategies employed in the studied BLDC system.

The simulations and results show that regenerative braking and rapid acceleration are achieved from the %SOC graphs. From speed graphs, the speed control of the BLDC motor is achieved at any load torques. The load sharing between the battery and supercapacitor is observed from the current graphs of both devices, which didn't violate the specified current limits. The load on the battery is decreased, leading to longer life and cyclability.

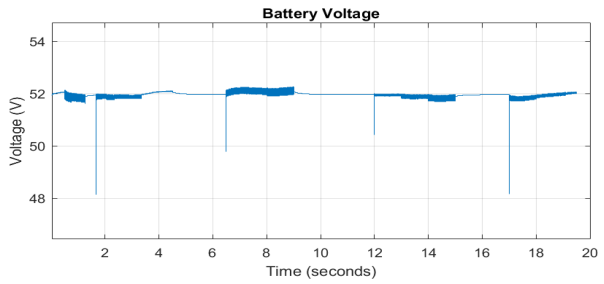

Fig. 10. Voltage at the battery.

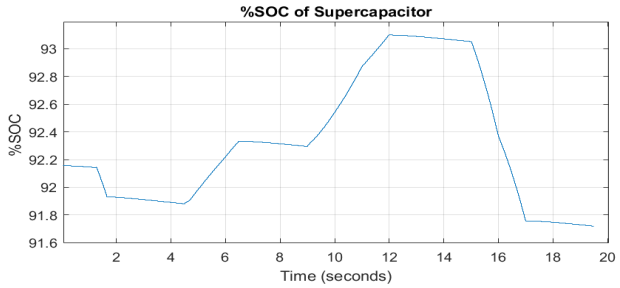

Fig. 11. %SOC of supercapacitor.

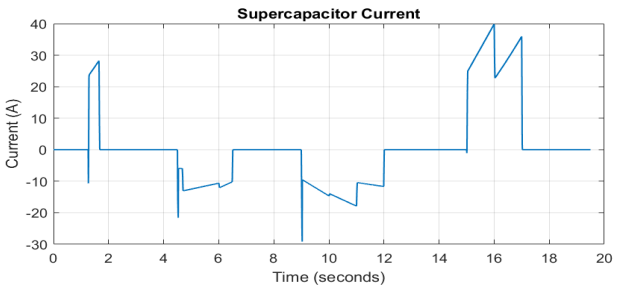

Fig. 12. Current in supercapacitor.

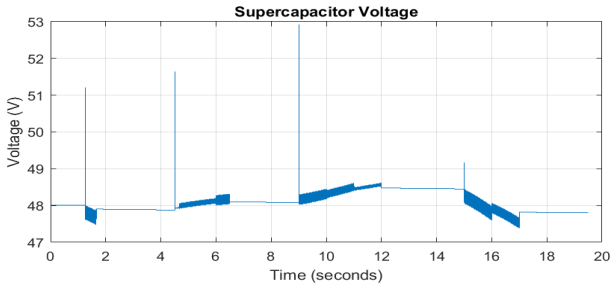

Fig. 13. Voltage at supercapacitor.

VI. Conclusion

The work is to design a system for regenerative braking and rapid acceleration by integrating supercapacitor and battery technology. This is achieved by combining a power inverter, logic circuits, and current and speed controllers to control the speed of a BLDC drive, as demonstrated in previous sections. Regenerative braking and rapid acceleration using the battery are depicted in graphs illustrating the battery's state of charge (SOC) and supercapacitor. Integration of supercapacitor and Li-ion battery enables regenerative braking and rapid acceleration. The system is configured to handle high power conditions with the supercapacitor and normal low power conditions with the battery, as evidenced by graphs showing currents in both components.

This work holds great potential for optimization. Switching current transients can be addressed with thermistors and inrush current limiter circuits. Mechanical aspects of the vehicle, such as air resistance, friction, and elevation, can be simulated and converted into load torques for more realistic testing. An actual drive cycle as a reference speed can better mimic real-world conditions. Alternative control algorithms can also be considered for integrating the battery and supercapacitor.

References

[1] A. Berrueta, A. Ursúa, I. S. Martín, A. Eftekhari, and P. Sanchis, "Supercapacitors: Electrical characteristics, modeling, applications, and future trends," *IEEE Access*, vol. 7, pp. 50 869–50 896, 2019.

[2] A. Khaligh and Z. Li, "Battery, ultracapacitor, fuel cell, and hybrid energy storage systems for electric, hybrid electric, fuel cell, and plug-in hybrid electric vehicles: State of the art," *IEEE Transactions on Vehicular Technology*, vol. 59, no. 6, pp. 2806–2814, 2010.

[3] X. Nian, F. Peng, and H. Zhang, "Regenerative braking system of electric vehicle driven by brushless dc motor," *IEEE Transactions on Industrial Electronics*, vol. 61, no. 10, pp. 5798–5808, 2014.

[4] M.-E. Choi, S.-W. Kim, and S.-W. Seo, "Energy management optimization in a battery/supercapacitor hybrid energy storage system," *IEEE Transactions on Smart Grid*, vol. 3, no. 1, pp. 463–472, 2012.

[5] J. Cao and A. Emadi, "A new battery/ultracapacitor hybrid energy storage system for electric, hybrid, and plug-in hybrid electric vehicles," *IEEE Transactions on Power Electronics*, vol. 27, no. 1, pp. 122–132, 2012.

[6] F. Naseri, E. Farjah, and T. Ghanbari, "An efficient regenerative braking system based on battery/supercapacitor for electric, hybrid, and plug-in hybrid electric vehicles with bldc motor," *IEEE Transactions on Vehicular Technology*, vol. 66, no. 5, pp. 3724–3738, 2017.

[7] P. Bathala, B. S. Srivasthav, Y. Sai Srinivas Reddy, and K. Deepa, "Estimation of regenerative braking force in electric vehicles for maximum energy recovery," in *2020 IEEE 17th India Council International Conference (INDICON)*, 2020, pp. 1–7.

[8] L. Solero, A. Lidozzi, and J. Pomilio, "Design of multiple-input power converter for hybrid vehicles," *IEEE Transactions on Power Electronics*, vol. 20, no. 5, pp. 1007–1016, 2005.